Numerical Modelling and Analysis of the Burning Transient in a Solid-Propellant Micro-Thruster

J.A. Moríñigo* and J. Hermida-Quesada**

National Institute for Aerospace Technology
* Dept. of Space Programmes, morignigoja@inta.es
** Dept. Aerodynamics and Propulsion, hermidaj@inta.es
Ctra. Ajalvir km.4, Torrejón de Ardoz 28850, Madrid, Spain

ABSTRACT

This work investigates an architecture of arrayed micro-thrusters of submillimeter size for spacecraft propulsion. Each single thruster comprises a setup of micro-channels arranged around the solid-propellant reservoir, hence initial heating of both sides of its wall by the hot gas takes place in the transient. Simulation of the unsteady response of the gas and wafer during the grain burning has been conducted under a multiphysics-based approach that fully couples the parts involved and focuses on the early phase of the transient. Preliminary results suggest the beneficial role played by the thermal management provided by the micro-channels, that mitigates the heat loss across the wall. Thus, miniaturization of the propellant reservoir within the submillimeter range is favoured due to the sustainment of higher temperatures ahead of the burning front, by the inner wall. Simulated firings show encouraging performance.

Keywords: combustion in microscale, MEMS, micro-thruster, multiphysics modelling.

1 INTRODUCTION

Two fundamental aspects are inherent to gas flows in propulsion-MEMS: their very low Reynolds numbers, hence turbulence is inhibited; and the high heat loss to the surrounding substrate, because of the large area to volume ratio. It is well known that the use of solid-propellant is advantageous as it provides no moving parts and simplicity to micro-thruster design. In addition, the sizing of arrays of μ-thrusters allows to meet the requirements of very small spacecrafts [1]. Nevertheless, the efficient conversion of the propellant chemical energy into thermal energy in the microscale remains a challenge for this class of micro-systems. To this respect, Rossi *et al*. [2,3] have analysed a variety of reservoir configurations filled with energetic materials and prope-llants. They have identified that thermal loss is responsible of the flame extinction at reservoir sizes of about a millimeter, where combustion becomes unstable or not sustained anymore. Kondo *et al*. [4] reported for a submillimeter rocket tested in vacuum, that the reservoir depressurization at the ignition phase leads to a low rate of success in the combustion starting and thrust generation.

Besides an adequate choice of propellant compositions, the thermal management of the energy released by the combustion influences to a great extent the performance, thus design optimization compatible with microfabrication is of paramount importance. For brevity, this paper presents preliminary results of the thermal management provided by a passage of μ-channels, here referred to as the *heating channels*, intended to thermally isolate the combustion zone and to enhance the heating of the inner walls. The micro-thruster arquitecture investigated is sketched in Fig. 1.

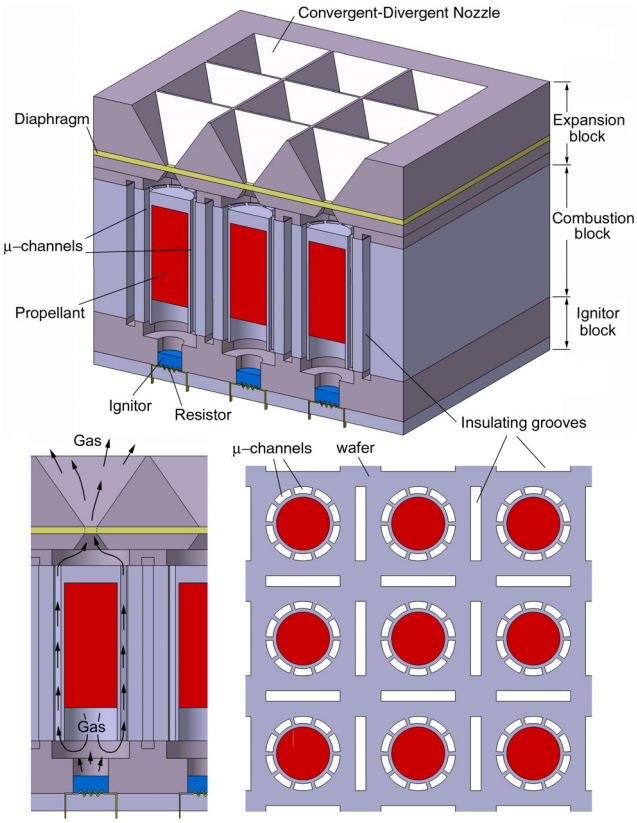

Figure 1: Schematics of a 3x3 array of solid-propellant micro-thruster with *heating channels*. Upper: general view with its first row sectioned; lower: meridian view with flow path indicated and cross-section of combustion block.

NSTI-Nanotech 2008, www.nsti.org, ISBN 978-1-4200-8505-1 Vol. 3

2 APPROACH

The computational domain used for the performance assessment is depicted in Fig. 2 for two locations of the propellant front. The passages sizing, of 30μm height, is conservative and compatible with the expected unburned particles sizes reported by other authors. The numerical simulations have been conducted under a multiphysics approach with thermal-fluid coupling between the gas and solids (wafer and propellant) involved. A continuum description of the gas flow based on the Navier-Stokes (NS) equations for laminar, compressible, heat conducting ideal gas is adopted at the microscale. The set of governing equations is solved in axisymmetric form with the FLUENT code, discretized according to a 2nd-order upwind algorithm and supplemented with a 2nd-order slip-flow model [5,6] for the velocity slip and temperature jump boundary conditions (BCs) at the nozzle wall to deal with the moderate rarefaction effects experienced by the gas. NS equations are solved in the gas zone in conjunction with the time-dependent heat diffusion equation in the solids. It is noted that heat conduction from the gas phase to the solid propellant (driven by the temperature normal gradient), is considered as the sole mechanism for ignition. Hence, radiative heat transfer is not included into the modelling, although it may enhance the decomposition rate of the propellant. The thermal balance at the burning surface (here simplified as non-moving and flat) to determine the surface temperature and instant of ignition (T_w=T_{ign}), states

$$-k_p \nabla T \cdot \vec{n} = \rho_p r_p q_p + \phi_f + \phi_{ign} \qquad (1)$$

being k_p the thermal conductivity of the propellant, q_p the heat released at the surface, ϕ_f the heat flux from the flame and ϕ_{ign} the heat flux from the igniter gas. Other issue of relevance included into the model is a diaphragm rupture condition, applied at the throat section to model the dynamics of the starting pressurization into the fluid cavity caused by the igniter firing prior to the diaphragm bursting. Solid-fluid coupling, heat flux BCs at the gas-propellant and gas-igniter interfaces, slip-flow BCs and diaphragm rupture have been coded in FLUENT as UDF routines. One basic criterion for propellant selection derives from the constrains to its use in actual small spacecrafts. In this work, GAP (Glycidyle Azide Polymer) -based propellant is assumed, suited for microsystems due to its homogeneity and ease of injection properties. The simulations mimic the propellant decomposition provoked by a pyrotechnic paste of ZPP (Zirconium Potassium Perchlorate: ρ=3570kg/m^3, T_f=5018ºK, burn rate (in mm/s): r=ap^n, with a=1.85·10^{-4} mm/s/Pa^{-n}, n=0.79, p in Pascal), as depicted in Fig. 1 and set at the lefthand boundary in Fig. 2, to ignite the GAP by providing a high temperature flux. This mechanism has been tested [2] and seems effective to achieve the opening of the nozzle to the near-vacuum ambient. The igniter-BC is modelled with a time dependent massflux law ρr at the adiabatic flame temperature. Albeit the ZPP and propellant products have different composition, it is assumed that thermodynamics and transport properties are identical and the composition is frozen (see Table 1).

GAP-based propellant:	
Density, ρ_p	1528 kg/m^3
Flame temperature, T_f	1991ºK
Auto-ignition temperature, T_{ign}	573ºK
Burn rate (in mm/s), r_p=ap^n	a=1.1mm/s/bar^{-n}, n=0.58
Products molecular weight, M	19.7 g/mol
Products specific heat, $C_{p,gas}$	2034 J/kg-K
Thermal conductivity, k_{gas}	0.16 W/m-K
Laminar viscosity, μ_{gas}	6.2 ·10^{-5} kg/m-K
Specific heats ratio, γ	1.26

Table 1: Propellant and combustion gas data

The high heat enthalpy of the igniter released during a very short time interval makes the gas velocity to become supersonic into the μ-channels and to generate shock waves that propagate downstream up to the diaphragm (Fig. 3). The small characteristic time inherent to this phenomenon requires an integration time step of about Δt~10^{-8}s to solve the pressure buildup at the ignition phase. Variation of the integration time-step is carried out in the explicit dual-time stepping method used.

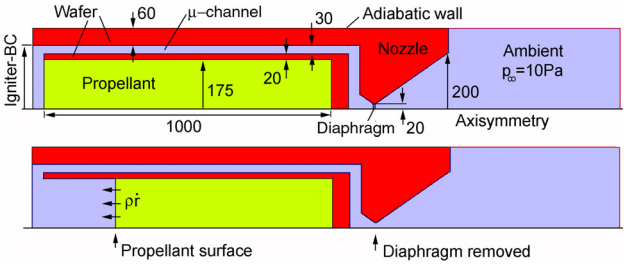

Figure 2: Computational domain of the axisymmetrical simulations (gas, wafer and propellant indicated). Upper: configuration before GAP ignition; lower: configuration at an intermediate instant of burning. Dimensions in μm.

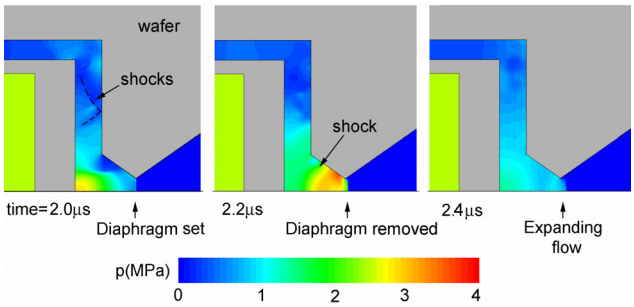

Figure 3: Time sequence of pressure snapshots focusing the diaphragm bursting due to the igniter flux at the early μs'.

3 RESULTS

The pressure peak visible in Fig. 4 is conservative in the sense that the model does not take into account the fluid region filled with air until the diaphragm rupture. Then, since viscosity and thermal conductivity of the combustion gas is notably higher than that of air, pressure peaks will tend to decrease due to the excess of viscous dissipation. After the ZPP flux extinction, steady pressure into the reservoir is rapidly settled down. Interestingly, this pressure level exhibits a significant dependence on the igniter flux lasting (t_{ign}), as it is seen in Fig.4. Regarding this behaviour, it should be noted that the burning surface area to the throat area ratio (A_p/A_{th}) drives the operating pressure p_c according to the steady approximation

$$p_c^{1-n} = \frac{a\rho_p}{\Gamma}\frac{A_p}{A_{th}}\sqrt{R_g T_t}\,, \quad \Gamma = \sqrt{\gamma}\left(\frac{2}{\gamma+1}\right)^{\frac{\gamma+1}{2(\gamma-1)}} \qquad (2)$$

where T_t denotes the averaged stagnation temperature at the nozzle inlet and determines the maximum massflow rate passing through the throat for prescribed geometry and ballistics. In fact, the steady p_c plotted in Fig.4 corresponds to the situation $T_t << T_f$, caused by the heat loss into the wafer and grain at large times of the transient. This thermally induced response is not addressed here in detail, requiring further investigation.

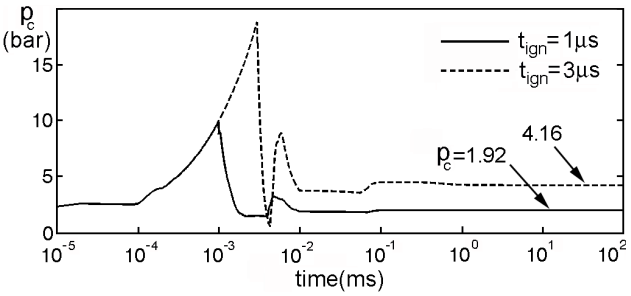

Figure 4: History of averaged pressure into the propellant reservoir for a ZPP heat flux lasting for 1 and 3μs.

Once the grain ignites, the reservoir wall temperature rises due to the heat flux at both sides and its head-end. This increase is illustrated in Fig. 5 for the startup time interval of 3ms, in which the propellant surface recedes a distance about twice the wall thickness (20μm) according to the burning rate law (1.6mm/s at 2bar). For t_{ign}=3μs, the hot gas penetrates further into the μ-channels because of its higher pressure. It is pointed out that the assumption of non-moving surface is only valid for short times after the reference instant corresponding to the surface location.

The thermal response of the μ-thruster shown in Fig. 6 corresponds to 90ms after the ignition and has been computed with the second propellant configuration depicted in Fig. 2. The temperature map shows that the hot gas at the μ-channel inlet enhances the heating of the portion of the reservoir wall ahead of the propellant, though a significant temperature decay occurs downstream the burning front near the wall. Nevertheless, the local temperature in this region remains over the propellant auto-ignition limit, thus it favours the sustainment of the chemical reactions. The progressive cooling of the gas inside the μ-channel is apparent, as well as the drop in stagnation temperature due to the heat transfer, which scales with the difference of the core temperature to the wall temperature, and leads to the bulk temperature T_t~450K upstream the nozzle inlet. Besides, the stagnation pressure drop along the μ-channel is small, under 9%. It is obvious that high p_c is beneficial as it enhances the heating rate at the early phase of the transient and because implies higher thrust delivered. However, the large surface area-to-volume ratio entails a penalty on the specific impulse derived from a lower T_t, which is likely unavoidable. An observation should be pointed out: even with T_t~300K, (cold flow), the smaller molecular mass of the expanding gas would imply a net gain of specific impulse compared with other gases (for instance, more than 27% in the case of N_2).

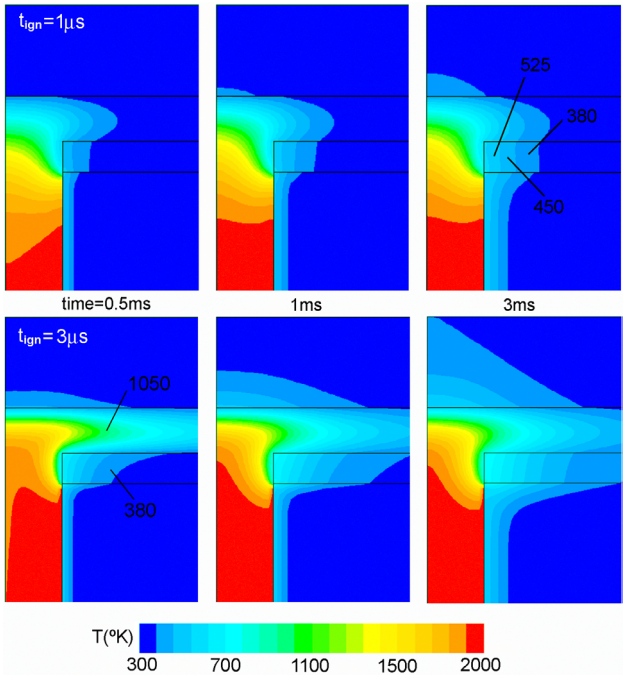

Figure 5: Sequence of temperature maps by the reservoir wall at 0.5, 1 and 3ms after the propellant ignition, for t_{ign}=1μs (upper row) and 3μs (lower row).

The determination of the gas film coefficient h_g in the μ-channels out of the computed flowfield at the beginning and intermediate time instants of the transient, yields values ranging from 1600 to 2800W/m^2-K (with Reynolds number Re=90 and 180, respectively and referred to the channel hydraulic diameter). A quantification of its effect on the thermal exchange is shown in Fig.7 for the propellant reservoir with and without *heating channels*. The averaged

NSTI-Nanotech 2008, www.nsti.org, ISBN 978-1-4200-8505-1 Vol. 3

T_w on the inner wall is plotted versus time for gas flow conditions at the μ-channel inlet taken from the NS simulations. The comparison of both configurations at the above mentioned h_g, is presented for two wafers made of silicon and glass. With μ-channels, the attained temperature rapidly raises beyond that without μ-channels. In particular, with a wafer of glass, the *heating channels* lead to a heating rate of about 50 to 80K per millisecond at the startup, which represents more than a twofold increase and stresses the improvement provided, at least at the early phase of the transient. Moreover, regarding the reservoir pressure, the gasdynamics equations show that the thermal exchange rate increases roughly linearly with it, so a moderate to high pressure in the reservoir is desirable.

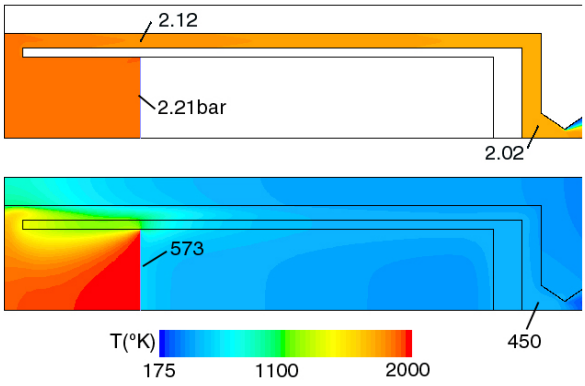

Figure 6: Stagnation pressure (upper) and temperature (lower) map after 90ms of burning transient.

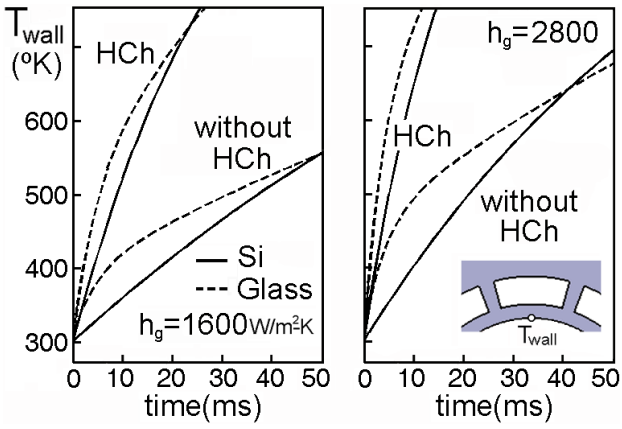

Figure 7: History of temperature on the inner wall of the propellant reservoir, with and without *heating channels* (HCh), made of silicon and glass.

4 CONCLUSIONS

The burning transient of a solid-propellant micro-thruster of submillimeter size with an arrangement of micro-channels around the propellant reservoir, has been simulated following a multiphysics-based approach. The modelling comprises high-speed flow, thermal coupling at the wafer-gas interface and burning surface, slip-flow at the nozzle wall, propellant ignition and diaphragm rupture at the beginning of the transient. The focus of the present investigation is not so much on the ignition times, but on the assessment of the unsteady thermal response of the micro-thruster setup here analysed. Preliminary simulations with GAP-based propellant and frozen composition have shown that the thermal management provided by the micro-channels during the transient reduces the heat loss and leads to the sustainment of higher temperatures in the reservoir. This aspect suggests the broadening of the flame extinction limits, thereby providing longer combustion times and the performance enhancement within the submillimeter range. The addition of a moving, non-flat recessing surface into a 3D model constitutes a next step and a challenge for more accurate predictions.

ACKNOWLEDGEMENT

This work was supported by the Spanish Ministry of Defence, as part of the micropropulsion activities in the Small Satellites Programme. The authors thank Emilio Lago-Llano of INTA for his assistance with some graphical material of this article.

REFERENCES

[1] Youngner D.W., Lu S.T., Choueiri E., Neidert J.B., Black III, R.E., Graham K.J., Fahey D., Lucus R. and Zhu X., "MEMS Mega-pixel Micro-thruster Arrays for Small Satellite Stationkeeping", in Proc. 14th Annual/USU Conference on Small Satellites, North Logan, USA, SSC00-X-2, 2000.

[2] Rossi C., Do Conto T., Estève D. and Larangôt B., "Design, Fabrication and Modelling of MEMS-based Microthruster for Space Application", Smart. Mater. Struct., 10:1156-1162, 2001.

[3] Rossi C., Briand D., Dumonteuil M., Camps Th., Quyên Pham Ph. and de Rooij N.F., "Matrix of 10x10 Addressed Solid Propellant Microthrusters: Review of the Technologies", Sensors & Actuators A, 126:241-252, 2006.

[4] Kondo K., Tanaka S., Habu H., Tokudome S., Hori K., Saito H., Itoh A., Watanabe M. and Esashi M., "Vacuum Test of a Micro-solid Propellant Rocket Array Thruster", IEICE Electronics Express, 1(8): 222-227, 2004.

[5] Zhang K.L., Chou S.K. and Ang S.S., "Performance Prediction of a Novel Solid-Propellant Micro-thruster", J. Prop. Power, 22(1):56-63, 2006.

[6] Moríñigo J.A, Hermida Quesada J. and Caballero Requena F., "Slip-Model Performance for Under-expanded Micro-scale Rocket Nozzle Flows", J. Thermal Science, 16(3):223-230, 2007.